

We are IntechOpen, the world's leading publisher of Open Access books Built by scientists, for scientists

6,900

Open access books available

186,000

International authors and editors

200M

Downloads

Our authors are among the

154

Countries delivered to

TOP 1%

most cited scientists

12.2%

Contributors from top 500 universities



WEB OF SCIENCE™

Selection of our books indexed in the Book Citation Index
in Web of Science™ Core Collection (BKCI)

Interested in publishing with us?
Contact book.department@intechopen.com

Numbers displayed above are based on latest data collected.
For more information visit www.intechopen.com



Combined Gravity or Self-Potential Anomaly Formula for Mineral Exploration

Khalid S. Essa and Mahmoud Elhussein

Abstract

A combined gravity and/or self-potential anomaly formula is utilized to estimate the model parameters of the buried geologic structures represented by simple geometric. The simple geometric shapes (spheres, cylinders, and sheets) are not really found but often applied to reduce the nonuniqueness in interpreting the gravity and self-potential data. Numerous approaches through the combined formula such as least squares, Werner deconvolution, and the particle swarm optimization method are used. The application of these methods was demonstrated by applying a synthetic gravity and self-potential example without and with 10% random noise to compare their efficiency in estimating the model parameters of the buried structures. Besides, they were applied to two field data for mineral exploration. The appraised model parameter values from each method were compared together and with those published in literature.

Keywords: gravity and/or self-potential, model parameters, noise, mineral exploration

1. Introduction

Minerals exploration is vital in many countries to increase the income of their people and their economy relies upon discovering minerals. The minerals or ores mined have different variety according to its important in the economy. Geophysical passive method such as gravity and self-potential play an important role in discovering these minerals or ores [1–5]. The gravity method based on measuring the variations in the Earth's gravitational field resulting from the density differences between the subsurface rocks while the self-potential method depended on the electrical potential that develops on the earth's surface due to flow of the natural electrical current on the subsurface [6, 7]. The interpretation of gravity and self-potential data falls on the main two categories as follows: the first category depends on three-dimensional and two-dimensional data elucidation [8–13], the second category is depending using the simple geometric-shaped model such as spheres, cylinders, and sheets which are playing a vital role in interpreting the subsurface structures to reach the priors information that help in more investigations [14–20]. In addition, methods depend on the global optimization algorithms such as genetic algorithm [21–24], particle swarm [25, 26], simulated annealing [27–32], flower pollination [33], memory-based hybrid dragonfly [34], differential evolution [35, 36].

Here, a combined formula for both gravity and self-potential [37] is applied to construct this chapter. Moreover, this formula is used to calculate the buried model parameters, for example in case of self-potential data, the parameters are the electric dipole moment or the amplitude coefficient (K), the polarization angle (θ), the depth (z), the shape (q), and the origin location (x_o) while in case of gravity data, the parameters are the amplitude coefficient (K), the depth (z), the shape (q), and the origin location (x_o) for the buried simple-geometric shapes. Three approaches are suggested to interpret the gravity or self-potential anomaly profile through the combined formula. These methods are least squares, Werner deconvolution, and the particle swarm optimization. The advantage of each method is demonstrated by applying a synthetic example for gravity and self-potential data without and with a 10% random noise to compare their efficiency in deducing the buried model parameters. In addition, they tested on two field example for mineral exploration.

2. The suggested combined gravity or self-potential formula

Firstly, the gravity anomaly formula due to simple geometric shapes is [15, 16, 18]

$$g(x_i, z, q) = K \frac{z^m}{\left((x_i - x_o)^2 + z^2\right)^q}. \quad (1)$$

Secondly, the self-potential anomaly formula for the same simple geometric models is [14]

$$V(x_i, z, \theta, q) = K \frac{xcos\theta + zsin\theta}{\left((x_i - x_o)^2 + z^2\right)^q}. \quad (2)$$

In Refs. [1, 37], Eqs. (1) and (2) were used to join together to produce a combined gravity or self-potential formula for the simple geometric structures such as a semi-infinite vertical cylinder, a dike, a horizontal cylinder, and a sphere (**Figure 1**) as follows:

$$J(x_i) = K \frac{cx_i(cos\theta)^n + z^p(sin\theta)^m}{\left((x_i - x_o)^2 + z^2\right)^q}, \quad (3)$$

where K is the amplitude coefficient, which depends on the shape of the buried model, z is the depth, θ is the polarization angle, x_i is the horizontal coordinates, x_o is the origin location of the buried structure, q is the shape (i.e., equals 1.5 for a sphere, 1.0 for a horizontal cylinder, and 0.5 for a semi-infinite vertical cylinder), c , n , p , and m are constants, which depend on the shape [37]. Eq. (3) is the combined formula for interpreting gravity or self-potential data. So, three suggested approaches were applied to estimate the unknown model parameters as follows:

2.1 The least-squares approach

Essa [37] developed this approach, which was relied on solving the problem of finding the depth from the measured data by solving a nonlinear form $F(z) = 0$ by minimizing it in a least-squares sense. After that, the estimated depth was used in estimating other parameters (the polarization angle and the dipole moment for

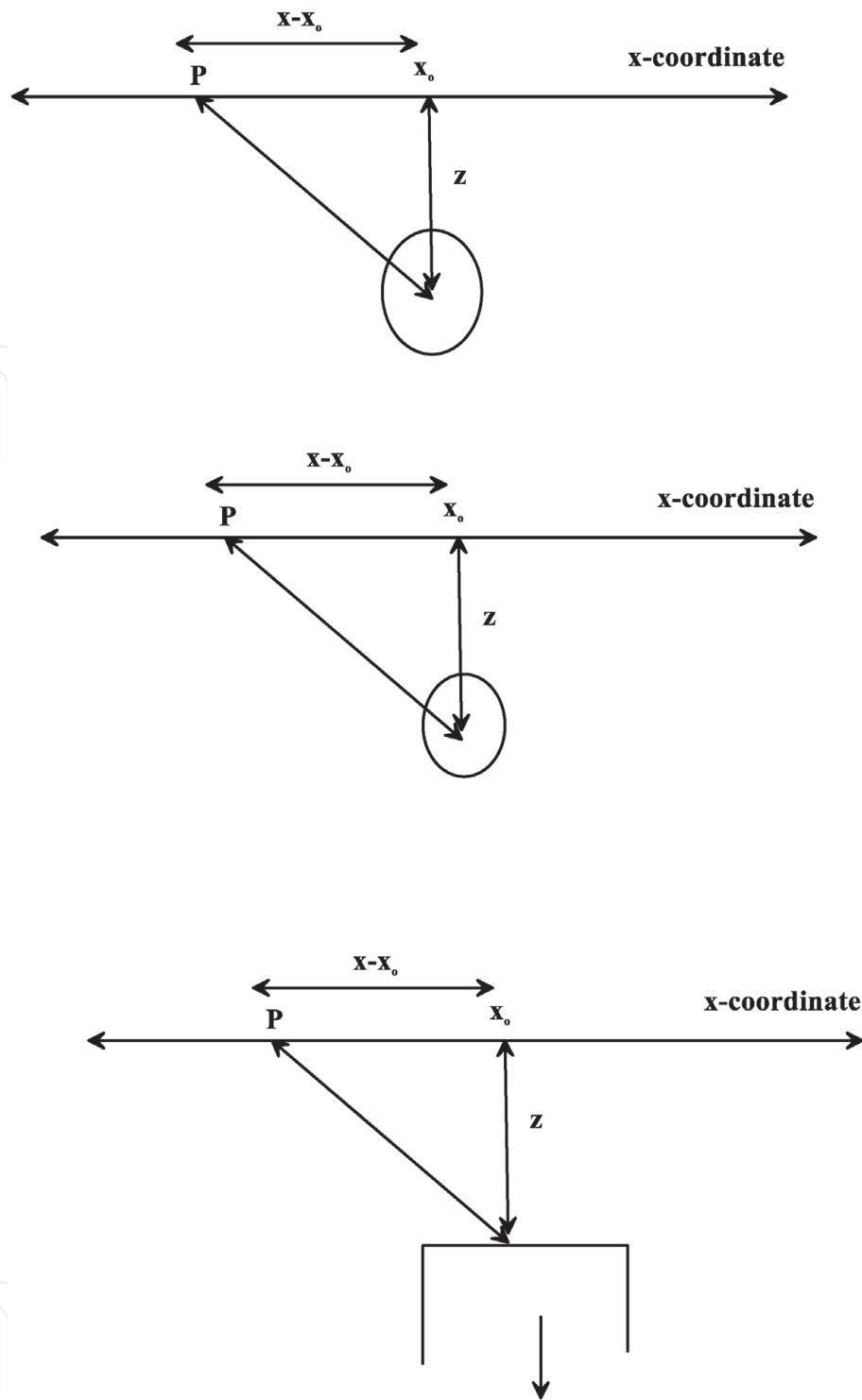


Figure 1. A sketch diagram for the simple geometric bodies as follows: a sphere model (top panel), a horizontal cylinder model (middle panel), and a semi-infinite vertical cylinder model (bottom panel).

self-potential data or the amplitude coefficient for gravity data) via suggesting the shape of the buried structure (the semi-infinite vertical cylinder, the dike, the horizontal cylinder and the sphere) at the lowest root-mean-squared error. This approach is a semi-automatic because that need assuming the shape of the buried structures (a priori information needed) and applied all observed points in estimating the model parameters.

2.2 Werner deconvolution approach

Werner deconvolution was proposed by Werner in 1953 [38]. This approach is used to estimate mainly the origin location and the depth of the buried structures.

Werner proposed to transform the equation of unknown parameters into a rational function. Eq. (3) can be rewritten in linear form follow:

$$J(x_i) \left((x_i - x_o)^2 + z^2 \right)^q - Kcx_i(\cos\theta)^n + Kz^p(\sin\theta)^m = 0, \quad (4)$$

$$J(x_i) \left((x_i - e_1)^2 + e_2 \right)^q - e_3x_i + e_4 = 0, \quad (5)$$

where $e_1 = x_o, e_2 = z^2, e_3 = Kc(\cos\theta)^n, e_4 = Kz^p(\sin\theta)^m$.

Eq. (5) is linear form in the four variables $e_1, e_2, e_3,$ and $e_4,$ so that a mathematically unique solution can be found for them from evaluating the equation at four points by assuming the shape of the buried structure.

2.3 The particle swarm approach

The particle swarm was suggested by [39] and has many various applications, for example, in geophysics [40–42]. For more detail in this approach, you find it many published literature [43, 44]. The model parameters values of the unknowns are relied upon the objective function, so that every problem can be resolved. In this approach, the particles represent the parameter which we are invert. In the beginning, each particle has a location and velocity. After that each particle changes its location (P_{best}) at every iteration until reach the optimum location (J_{best}). This operation is done by using the following forms:

$$V_i^{k+1} = c_3V_i^k + c_1rand(P_{best} - x_i^{k+1}) + c_2rand(J_{best} - x_i^{k+1}), \quad (6)$$

$$x_i^{k+1} = x_i^k + V_i^{k+1}, \quad (7)$$

where v_i^k is the velocity of the particle i at the k th cycle, x_i^k is the current i modeling at the k th cycle, $rand$ is the random number between $[0, 1]$, c_1 and c_2 are positive constant numbers and equal 2, c_3 is the inertial coefficient which control the velocity of the particle and usually taken less than 1, x_i^k is the positioning of the particle i at the k th cycle.

The five source parameters ($K, z, \theta, x_o,$ and q) can be assessed by using the particle swarm approach on the subsequent objective function (Obj):

$$Obj = \sqrt{\frac{\sum_{j=1}^N (J_j^o - J_j^c)^2}{N}}, \quad (8)$$

where N is the data points number, J_j^o is the observed gravity or self-potential anomaly, and J_j^c is the estimated anomaly at the point x_j .

3. Synthetic example

To test the ability of each suggested approach in assessing the buried model parameters for the simple geometric shapes such as spheres, cylinders, and sheets. Two synthetic examples are suggested for these interpretation. First one is belonging to use the gravity data and second is applying the self-potential data.

3.1 Gravity anomaly model

A gravity anomaly of a horizontal cylinder model is generated using the following parameters $K = 200 \text{ mGal} \times \text{m}, z = 5 \text{ m}, x_o = 0, q = 1.0,$ and profile length = 100 m

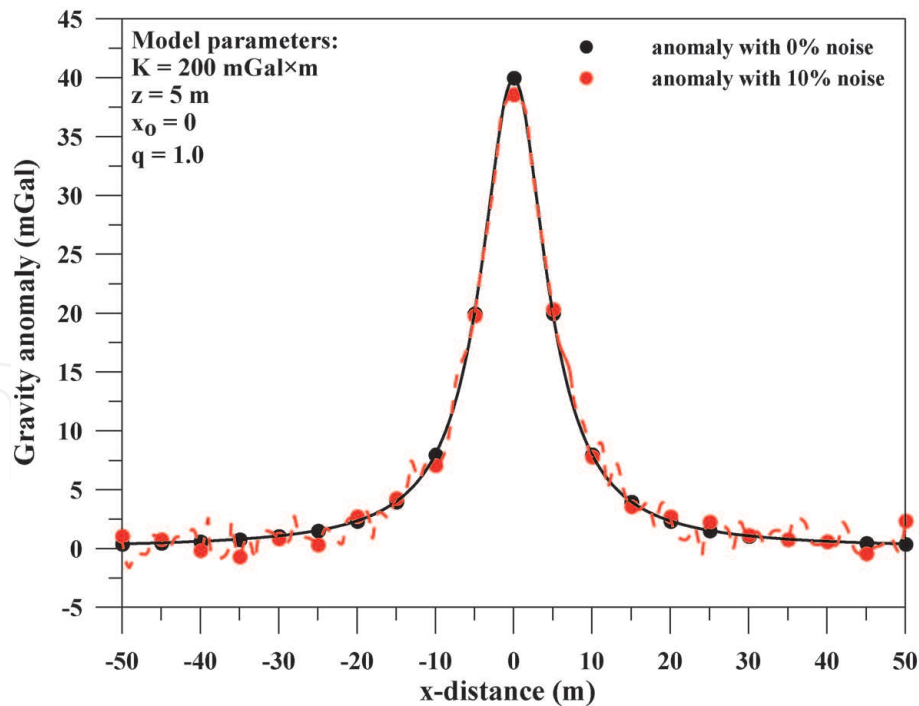


Figure 2. A gravity model due to horizontal cylinder without and with a 10% of random noise ($K = 200 \text{ mGal} \times \text{m}$, $z = 5 \text{ m}$, $x_0 = 0$, $q = 1$, and profile length = 100 m).

(Figure 2). The procedures of interpreting the forward model are done using three steps as follows:

First step: using the least-squares approach to interpret the gravity anomaly yielding from the above mentioned parameters for different s -values for the three suggested shape bodies, i.e., $q = 0.5$, $q = 1.0$, and $q = 1.5$, after that the RMS is

s-values (m)	$J(x_j)$ (mGal)	q = 0.5		q = 1.0		q = 1.5	
		K (mGal×m)	z (m)	K (mGal×m)	z (m)	K (mGal×m ²)	z (m)
For synthetic data with 0% noise							
+1	38.46	50	2.4	200	5	1100	6.5
-1	38.46						
+2	34.48						
-2	34.48						
+3	29.41						
-3	29.41						
+4	24.39						
-4	24.39						
Average		50	2.4	200	5	1100	6.5
RMS (mGal)		5.7		0		4.1	
For synthetic data with 10% noise							
+1	38.01	48.6	2.3	195.6	4.9	1086.6	6.4
-1	37.92						
+2	34.64						
-2	34.15						
+3	29.15						
-3	28.75						
+4	24.68						
-4	24.40						
Average		48.5	2.3	195.8	4.9	1084.6	6.4
RMS (mGal)		5.8		1.0		4.2	

Table 1. Numerical results using the least-squares approach for a gravity model due to horizontal cylinder without and with a 10% of random noise ($K = 200 \text{ mGal} \times \text{m}$, $z = 5 \text{ m}$, $x_0 = 0$, $q = 1$, and profile length = 100 m).

Type of body	Parameters	Used ranges	Result	RMS (mGal)
Horizontal cylinder model	For synthetic data with 0% noise			
	K (mGal×m)	100-700	200	0
	z (m)	2-12	5	
	q	0-3	1	
	x _o (m)	-20-50	0	
	For synthetic data with 10% noise			
	K (mGal×m)	100-700	197	0.12
	z (m)	2-12	4.9	
	q	0-3	1.01	
	x _o (m)	-20-50	0.01	

Table 2.

Numerical results using the particle swarm approach for a gravity model due to horizontal cylinder without and with a 10% of random noise ($K = 200 \text{ mGal}\times\text{m}$, $z = 5 \text{ m}$, $x_o = 0$, $q = 1$, and profile length = 100 m).

calculated to execute the best-fit parameters (happens at the lowest RMS) (Table 1). Second step: Werner deconvolution approach is utilized to infer the same gravity data. An 11 clustered solutions to determine in the average evaluated depth (4.9 m) (Figure 2). Third step: the particle swarm method is applied to obtain the parameters (Table 2).

Moreover, a 10% random noise added to the synthetic gravity data mentioned above (Figure 2) to test the efficiency of the suggested approaches in interpreting the gravity data. Also, the three approaches are used for this data as mentioned in

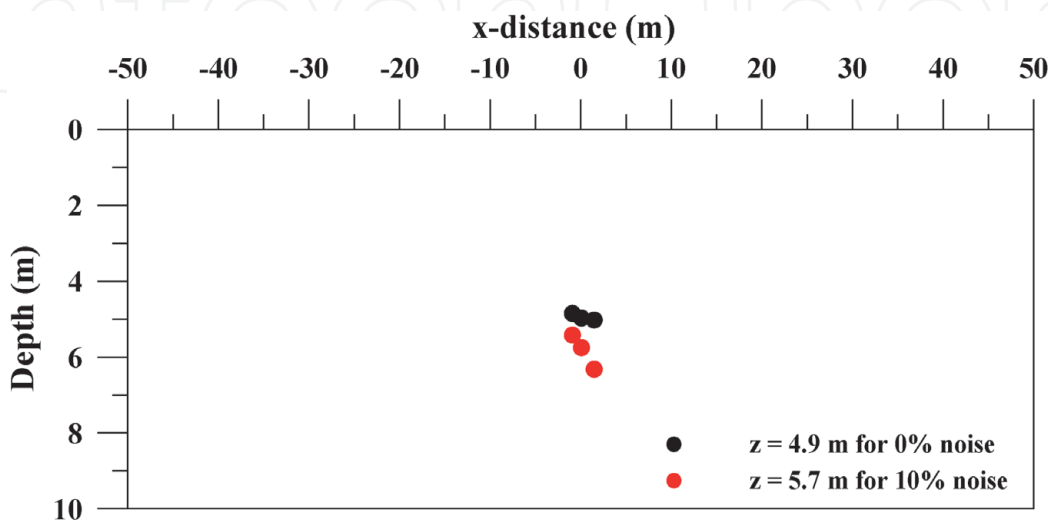


Figure 3.

Werner deconvolution solutions for a gravity model due to horizontal cylinder without and with a 10% of random noise ($K = 200 \text{ mGal}\times\text{m}$, $z = 5 \text{ m}$, $x_o = 0$, $q = 1$, and profile length = 100 m).

Table 1 (the least-squares approach results), **Figure 3** (Werner deconvolution results), and **Table 2** (the particle swarm results). Finally, the estimated parameters are in all case are in good agreement with the true parameters.

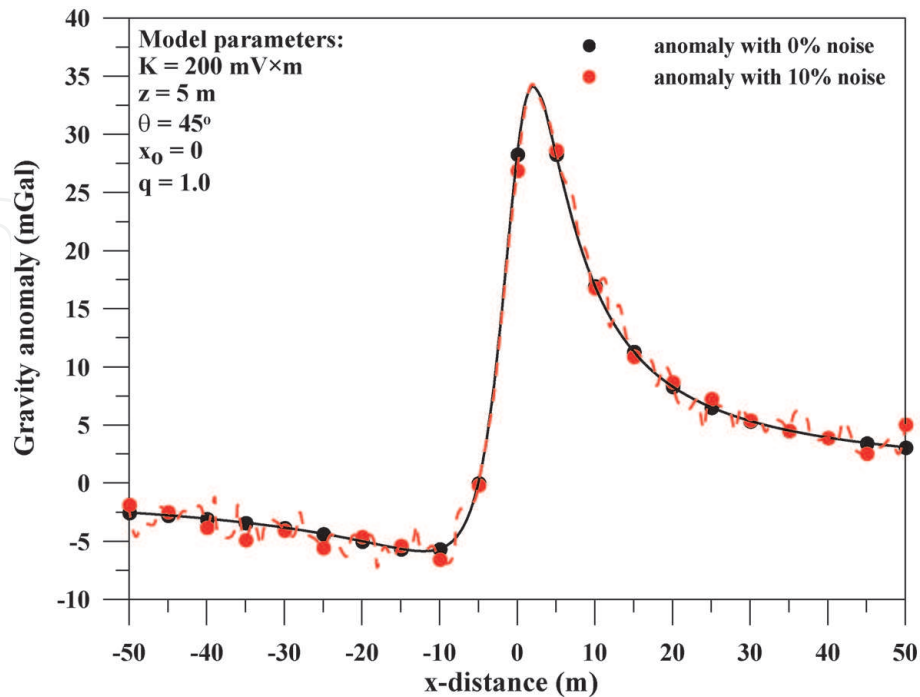


Figure 4. A self-potential model due to horizontal cylinder without and with a 10% of random noise ($K = 200 \text{ mV}\times\text{m}$, $z = 5 \text{ m}$, $\theta = 45^\circ$, $x_0 = 0$, $q = 1$, and profile length = 100 m).

s-values (m)	$J(x_i)$ (mV)	q = 0.5			q = 1.0			q = 1.5		
		K (mV)	z (m)	θ ($^\circ$)	K (mV×m)	z (m)	θ ($^\circ$)	K (mV×m ²)	z (m)	θ ($^\circ$)
For synthetic data with 0% noise										
+1	38.46	48.9	1.6	67.2	200	5	45	1565.3	6.4	29.7
-1	38.46									
+2	34.48									
-2	34.48									
+3	29.41									
-3	29.41									
+4	24.39									
-4	24.39									
Average		48.9	1.6	67.2	200	5	45	1565.3	6.4	29.7
RMS (mV)		12.8			0			4.1		
For synthetic data with 10% noise										
+1	38.01	46.5	1.5	64.8	192.3	4.8	42.1	1512.7	5.9	27.6
-1	37.92									
+2	34.64									
-2	34.15									
+3	29.15									
-3	28.75									
+4	24.68									
-4	24.40									
Average		46.9	1.5	65.6	195.8	4.9	4.8	1520.7	5.9	27.6
RMS (mV)		13.0			1.1			4.2		

Table 3. Numerical results using the least-squares approach for a self-potential model due to horizontal cylinder without and with a 10% of random noise ($K = 200 \text{ mV}\times\text{m}$, $z = 5 \text{ m}$, $\theta = 45^\circ$, $x_0 = 0$, $q = 1$, and profile length = 100 m).

3.2 Self-potential anomaly model

A self-potential anomaly of a horizontal cylinder model is generated using the following parameters $K = 200 \text{ mV}\times\text{m}$, $z = 5 \text{ m}$, $\theta = 45^\circ$, $q = 1.0$, and profile length = 100 m (Figure 4). The similar interpretation procedures mentioned above are used

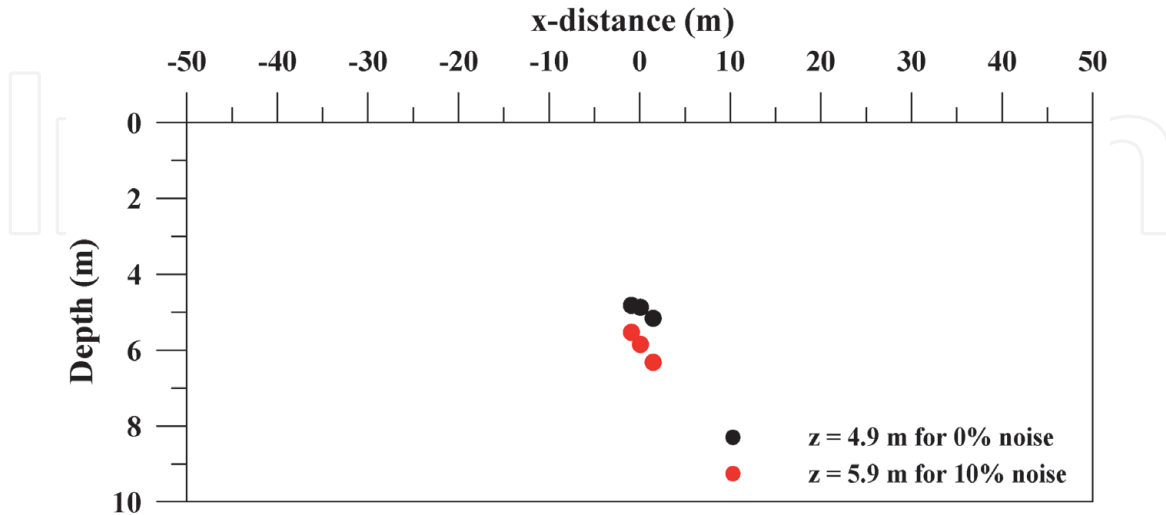


Figure 5. Werner deconvolution solutions for a self-potential model due to horizontal cylinder without and with a 10% of random noise ($K = 200 \text{ mV}\times\text{m}$, $z = 5 \text{ m}$, $\theta = 45^\circ$, $x_o = 0$, $q = 1$, and profile length = 100 m).

Type of body	Parameters	Used ranges	Result	RMS (mV)
Horizontal cylinder model	For synthetic data with 0% noise			
	K (mV×m)	100-700	200	0
	z (m)	2-12	5	
	θ (°)	5-85	45	
	q	0-3	1	
	x_o (m)	-20-50	0	
	For synthetic data with 10% noise			
	K (mV×m)	100-700	195	0.22
	z (m)	2-12	4.9	
	θ (°)	5-85	43.5	
q	0-3	0.98		
x_o (m)	-20-50	-0.02		

Table 4. Numerical results using the particle swarm approach for a self-potential model due to horizontal cylinder without and with a 10% of random noise ($K = 200 \text{ mV}\times\text{m}$, $z = 5 \text{ m}$, $\theta = 45^\circ$, $x_o = 0$, $q = 1$, and profile length = 100 m).

as follows: first, the least-squares approach is applied to interpret the self-potential data using various s -values for the three suggested shape bodies, i.e., $q = 0.5$, $q = 1.0$, and $q = 1.5$, after that the RMS is calculated to execute the best-fit parameters (happens at the lowest RMS) (**Table 3**). Secondly, the Werner deconvolution approach is utilized to infer the same self-potential data using 11 clustered solutions to determine in the average evaluated depth (4.9 m) (**Figure 5**). Third step: the particle swarm method is applied to obtain the parameters (**Table 4**). Besides, a 10% random noise was added to this data (**Figure 3**) to test the efficiency of the suggested approaches in interpretation. Furthermore, the results from applying the three approaches are mentioned in **Table 3** (the least-squares approach results), **Figure 5** (Werner deconvolution results), and **Table 4** (the particle swarm results). Finally, the estimated parameters are in all case are in good agreement with the actual parameters.

4. Field examples

The three suggested approaches have been organized to inspect the gravity and self-potential anomalies due to three simple bodies of various structures, e.g., sheets, cylinders, and spheres. Two mineral field examples from India and Turkey have been interpreted to study the reliability of the suggested approaches. The relevant model parameters (K , z , θ , x_0 , and q) are evaluated in an integrated way with the existing geological and geophysical results.

4.1 Gravity anomaly of manganese ore body

Figure 6 shows a gravity anomaly was collected over a manganese deposit near Nagpur, India [45]. This gravity profile has a length of 333 m and digitized with an interval of 27 m. This gravity anomaly is subjected to the three interpretation approaches as discussed earlier. Firstly, the interpreted results due to applying the least-squares approach are shown in **Table 5** for various s -values. Besides, the use of

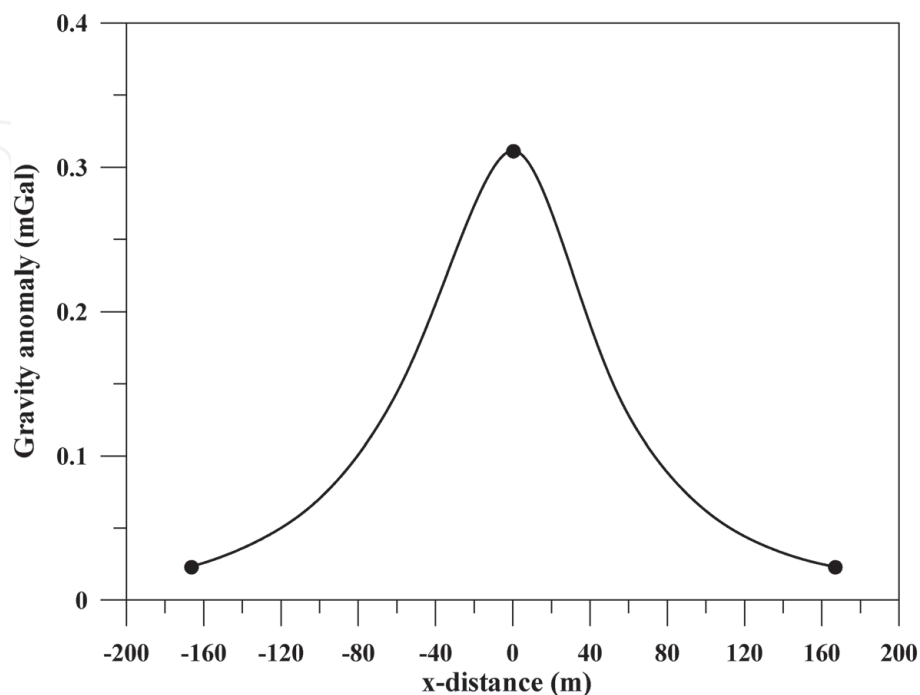


Figure 6.
A gravity anomaly due to a manganese ore body, India.

s-values (m)	J(x _j) (mGal)	q = 0.5		q = 1.0		q = 1.5	
		K (mGal×m)	z (m)	K (mGal×m)	z (m)	K (mGal×m ²)	z (m)
+27	0.225	124.6	18.4	24.8	63.2	342.4	112.8
-27	0.233						
+54	0.155	156.1	21.9	25.3	64.3	448.4	123.4
-54	0.139						
+81	0.095	178.3	25.7	22.1	57.4	456.2	124.1
-81	0.107						
Average		153	22	24.1	61.6	415.7	120.1
RMS (mGal)		40.3		2.7		6.2	

Table 5.
Numerical results using the least-squares approach for a manganese field example, India.

Type of body	Parameters	Used ranges	Result	RMS (mGal)
Horizontal cylinder model	K (mGal×m)	1-100	17.3	0.06
	z (m)	1-100	57.8	
	q	0-3	1.0	
	x ₀ (m)	-10-10	0.8	

Table 6.
Numerical results using the particle swarm approach for a manganese field example, India.

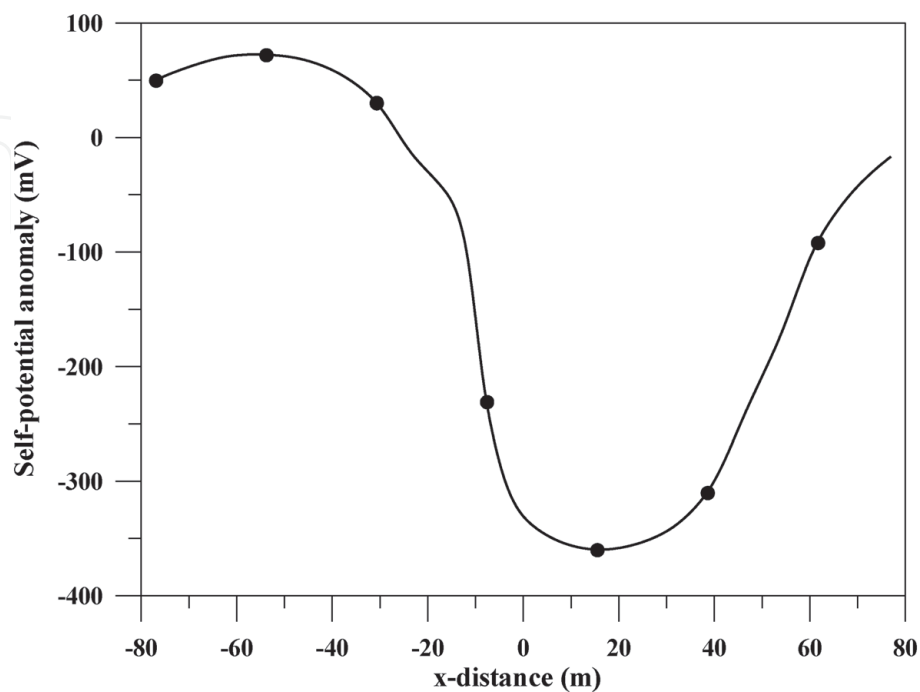


Figure 7.
A self-potential anomaly due to a Weiss copper ore body, Turkey.

s-values (m)	J(x _j) (mV)	q = 0.5			q = 1.0			q = 1.5		
		K (mV)	z (m)	θ (°)	K (mV×m)	z (m)	θ (°)	K (mV×m ²)	z (m)	θ (°)
+7.7	-352.81	-1148.3	18.4	72.4	-9876.2	63.2	54.6	-472589.6	28.7	38.4
-7.7	-230.57									
+15.4	-359.75	-1192.1	21.9	65.8	-10056.4	64.3	50.9	-471236.1	29.6	37.8
-15.4	-52.78									
+23.1	355.58	-1181.7	25.7	64.9	-9986.3	57.4	49.0	-470893.4	30.1	37.2
-23.1	-15.28									
Average		-1174.0	22.0	67.7	-9972.9	61.6	51.5	-471236.1	29.5	37.8
RMS (mV)		107.9			64.3			38.0		

Table 7.
 Numerical results using the least-squares approach for a Weiss copper field example, Turkey.

Type of body	Parameters	Used ranges	Result	RMS (mV)
Spherical model	K (mV×m ²)	-200000--500000	-471200.3	34.2
	z (m)	10-50	29.7	
	θ (°)	5-85	37.6	
	q	0-3	1.48	
	x _o (m)	-10-10	-2.3	

Table 8.
 Numerical results using the particle swarm approach for a Weiss copper field example, Turkey.

Werner deconvolution approach, the interpretive results obtained are $z = 56.8$ m and $x_o = 0.6$ m. Finally, the depth and the other model parameters evaluated by using the particle swarm approach are presented in **Table 6**.

4.2 Self-potential anomaly of manganese ore body

Figure 7 demonstrates a self-potential anomaly over a Weiss copper ore body in the Ergani copper district, Turkey [46]. The Weiss self-potential anomaly profile has a length of 144 m and digitized with an interval of 7.7 m. This anomaly has subjected to the three interpretation approaches as discussed earlier. Firstly, the interpreted results due to applying the least-squares approach are shown in **Table 7** for various s-values. Also, the applying of the Werner deconvolution approach, the interpretive results obtained are $z = 36.9$ m and $x_o = -2.1$ m. Finally, the depth and the other model parameters evaluated by using the particle swarm approach are presented in **Table 8**.

5. Conclusions

The three geophysical approaches (the least-squares approach, Werner deconvolution approach, and the particle swarm approach) discussed here to interpret gravity or self-potential data using a combined formula for the simple

geometric models (spheres, cylinders, and dikes) are stable and give a good results. The stability of these approaches has been confirmed and tested applying two synthetic examples with a 10% and without random noise and two field data for mineral explorations. The estimated parameters in all cases demonstrated the importance of these approaches in interpreting the gravity or self-potential data.

Acknowledgements

The authors would like to thank and express appreciation to Ms. Dolores Kuzelj, Author Service Manager, for her assistance and cooperation in this issue.

Conflict of interest

There is no conflict of interest.

Author details

Khalid S. Essa* and Mahmoud Elhussein
Faculty of Science, Geophysics Department, Cairo University, Giza, Egypt

*Address all correspondence to: khalid_sa_essa@yahoo.com

IntechOpen

© 2020 The Author(s). Licensee IntechOpen. This chapter is distributed under the terms of the Creative Commons Attribution License (<http://creativecommons.org/licenses/by/3.0>), which permits unrestricted use, distribution, and reproduction in any medium, provided the original work is properly cited. 

References

- [1] Essa KS. A generalized algorithm for gravity or self-potential data inversion with application to mineral exploration. In: 21th Geophysical conference and Exhibition; Sydney, New South Wales, Australia. 2010
- [2] Mehane S, Essa KS, Smith P. A rapid technique for estimating the depth and width of a two-dimensional plate from self-potential data. *Journal of Geophysics and Engineering*. 2011;**8**:447-456
- [3] Essa KS, Elhussein M. A new approach for the interpretation of self-potential data by 2-D inclined plate. *Journal of Applied Geophysics*. 2017; **136**:455-461
- [4] Essa KS. Minerals. Rijeka, Croatia: InTech d.o.o.; 2019. ISBN: 978-1-83962-682-1
- [5] Essa KS, Munschy M. Gravity data interpretation using the particle swarm optimization method with application to mineral exploration. *Journal of Earth System Science*. 2019;**128**:123
- [6] Sato M, Mooney HM. The electrochemical mechanism of sulfide self-potentials. *Geophysics*. 1960;**25**:226-249
- [7] Nettleton LL. Gravity and Magnetism in Oil Prospecting. New York: McGraw-Hill Book Co.; 1976
- [8] Zhang J, Zhong B, Zhou X, Dai Y. Gravity anomalies of 2D bodies with variable density contrast. *Geophysics*. 2001;**66**:809-813
- [9] Colangelo G, Lapenna V, Perrone A, Piscitelli S, Telesca L. 2D self-potential tomographies for studying groundwater flows in the Varco d'Izzo landslide (Basilicata, southern Italy). *Engineering Geology*. 2006;**88**:274-286
- [10] Minsley BJ, Sogade J, Morgan FD. Three-dimensional self-potential inversion for subsurface DNAPL contaminant detection at the Savannah River Site, South Carolina. *Water Resources Research*. 2007;**43**:W04429
- [11] Cai H, Xiong B, Zhu Y. 3D Modeling and Inversion of Gravity Data in Exploration Scale, Gravity—Geoscience Applications, Industrial Technology and Quantum Aspect. In: Zouaghi T, editor. Rijeka: IntechOpen; 2017. DOI: 10.5772/intechopen.70961
- [12] Biswas A. A review on modeling, inversion and interpretation of self-potential in mineral exploration and tracing paleo-shear zones. *Ore Geology Reviews*. 2017;**91**:21-56
- [13] Biswas A. In: Essa KS, editor. Inversion of Amplitude from the 2-D Analytic Signal of Self-Potential Anomalies, Minerals. Rijeka: IntechOpen; 2019. DOI: 10.5772/intechopen.79111
- [14] Essa KS, Mehane S, Smith P. A new inversion algorithm for estimating the best fitting parameters of some geometrically simple body from measured self-potential anomalies. *Exploration Geophysics*. 2008;**39**: 155-163
- [15] Essa KS. A fast least-squares method for inverse modeling of gravity anomaly profiles due simple geometric-shaped structures. In: Near Surface Geoscience 2012—18th European Meeting of Environmental and Engineering Geophysics; Paris, France. 2012
- [16] Essa KS. A fast interpretation method for inverse modelling of residual gravity anomalies caused by simple geometry. *Journal of Geological Research*. 2012;**2012**: Article ID 327037
- [17] Biswas A, Sharma SP. Resolution of multiple sheet-type structures in

self-potential measurement. *Journal of Earth System Science*. 2014;**123**:809-825

[18] Essa KS. New fast least-squares algorithm for estimating the best-fitting parameters due to simple geometric-structures from gravity anomalies. *Journal of Advanced Research*. 2014; **5**(1):57-65

[19] Biswas A, Sharma SP. Interpretation of self-potential anomaly over idealized body and analysis of ambiguity using very fast simulated annealing global optimization. *Near Surface Geophysics*. 2015;**13**:179-195

[20] Mehane S, Essa KS. 2.5D regularized inversion for the interpretation of residual gravity data by a dipping thin sheet: Numerical examples and case studies with an insight on sensitivity and non-uniqueness. *Earth, Planets and Space*. 2015;**67**:130

[21] Di Maio R, Rani P, Piegari E, Milano L. Self-potential data inversion through a Genetic-Price algorithm. *Computers & Geosciences*. 2016;**94**: 86-95

[22] Di Maio R, Piegari E, Rani P. Source depth estimation of self-potential anomalies by spectral methods. *Journal of Applied Geophysics*. 2017;**136**:315-325

[23] Di Maio R, Piegari E, Rani P, Avella A. Self-potential data inversion through the integration of spectral analysis and tomographic approaches. *Geophysical Journal International*. 2016; **206**:1204-1220

[24] Di Maio R, Piegari E, Rani P, Carbonari R, Vitagliano E, Milano L. Quantitative interpretation of multiple self-potential anomaly sources by a global optimization approach. *Journal of Applied Geophysics*. 2019;**162**:152-163

[25] Singh A, Biswas A. Application of global particle swarm optimization for

inversion of residual gravity anomalies over geological bodies with idealized geometries. *Natural Resources Research*. 2016;**25**:297-314

[26] Essa KS, Elhussein M, Youssef MA. Magnetic data interpretation using new techniques: A comparative study. In: Biswas A, Sharma S, editors. *Advances in Modeling and Interpretation in Near Surface Geophysics*, Springer Geophysics. Cham: Springer; 2020. pp. 263-294

[27] Sharma SP, Biswas A. Interpretation of self-potential anomaly over a 2D inclined structure using very fast simulated-annealing global optimization—An insight about ambiguity. *Geophysics*. 2013;**78**:WB3-WB15

[28] Biswas A, Sharma SP. Optimization of self-potential interpretation of 2-D inclined sheet-type structures based on very fast simulated annealing and analysis of ambiguity. *Journal of Applied Geophysics*. 2014;**105**:235-247

[29] Biswas A. Interpretation of gravity and magnetic anomaly over thin sheet-type structure using very fast simulated annealing global optimization technique. *Modeling Earth Systems and Environment*. 2016;**2**:30

[30] Biswas A, Sharma SP. Interpretation of self-potential anomaly over 2-D inclined thick sheet structures and analysis of uncertainty using very fast simulated annealing global optimization. *Acta Geodaetica et Geophysica*. 2017;**52**:439-455

[31] Biswas A, Parija MP, Kumar S. Global nonlinear optimization for the interpretation of source parameters from total gradient of gravity and magnetic anomalies caused by thin dyke. *Annals of Geophysics*. 2017;**60**: G0218

[32] Biswas A. Inversion of source parameters from magnetic anomalies

for mineral/ore deposits exploration using global optimization technique and analysis of uncertainty. *Natural Resources Research*. 2018;**27**:77-107

[33] Sungkono. Robust interpretation of single and multiple self-potential anomalies via flower pollination algorithm. *Arabian Journal of Geoscience*. 2020;**13**:100

[34] Ramadhani I, Sungkono S. A new approach to model parameter determination of self-potential data using memory-based hybrid dragonfly algorithm. *International Journal on Advanced Science, Engineering and Information Technology*. 2019;**9**: 1772-1782

[35] Ekinici YL, Balkaya Ç, Göktürkler G. Parameter estimations from gravity and magnetic anomalies due to deep-seated faults: Differential evolution versus particle swarm optimization. *Turkish Journal of Earth Sciences*. 2019;**28**: 860-881

[36] Ekinici YL, Balkaya Ç, Göktürkler G. Global optimization of near-surface potential field anomalies through metaheuristics, advances in modeling and interpretation in near surface geophysics. In: Biswas A, Sharma S, editors. *Springer Geophysics*. Cham: Springer; 2020. pp. 155-188

[37] Essa KS. A new algorithm for gravity or self-potential data interpretation. *Journal of Geophysics and Engineering*. 2011;**8**:434-446

[38] Werner S. Interpretation of magnetic anomalies at sheet like bodies. *Sveriges Geologiska Undersok, Series C, Arsbok*. 1953;**43**(6):413-449

[39] Kennedy J, Eberhart R. *Particle Swarm Optimization: IEEE International Conference on Neural Networks (Perth, Australia)*. Vol. IV. Piscataway, NJ: IEEE Service Center; 1995. pp. 1942-1948

[40] Essa KS. A particle swarm optimization method for interpreting self potential anomalies. *Journal of Geophysics and Engineering*. 2019;**16**: 463-477

[41] Essa KS. Self potential data interpretation utilizing the particle swarm method for the finite 2D inclined dike: Mineralized zones delineation. *Acta Geodaetica et Geophysica*. 2020. DOI: 10.1007/s40328-020-00289-2

[42] Essa KS, Elhoussein M. Interpretation of magnetic data through particle swarm optimization: Mineral exploration cases studies. *Natural resources Research*. 2020;**29**:521-537

[43] Santos FAM. Inversion of self-potential of idealized bodies anomalies using particle swarm optimization. *Computers & Geosciences*. 2010;**36**: 1185-1190

[44] Essa KS, Elhoussein M. PSO (particle swarm optimization) for interpretation of magnetic anomalies caused by simple geometrical structures. *Pure and Applied Geophysics*. 2018;**175**:3539-3553

[45] Reddi AGB, Murthy BSR, Kesavanani MA. *Compendium of Four Decades of Geophysical Activity in Geological Survey of India*. GSI Special Publication No. 36. Geological Survey of India; 1995

[46] Yungul S. Interpretation of spontaneous polarization anomalies caused by spherical ore bodies. *Geophysics*. 1950;**15**:237-246